Fatigue Crack Growth Monitoring of Idealized Gearbox Spline Component using Acoustic Emission

Lu Zhang[a], Didem Ozevin*[a], William Hardman[b], Seth Kessler[c], Alan Timmons[b]
[a]Civil and Materials Engineering, University of Illinois at Chicago, Chicago IL; [b]NAVAIR NAS Patuxent River MD; [c]Metis Design Corporation, Boston MA

ABSTRACT

The spline component of gearbox structure is a non-redundant element that requires early detection of flaws for preventing catastrophic failures. The acoustic emission (AE) method is a direct way of detecting active flaws; however, the method suffers from the influence of background noise and location/sensor based pattern recognition method. It is important to identify the source mechanism and adapt it to different test conditions and sensors. In this paper, the fatigue crack growth of a notched and flattened gearbox spline component is monitored using the AE method in a laboratory environment. The test sample has the major details of the spline component on a flattened geometry. The AE data is continuously collected together with strain gauges strategically positions on the structure. The fatigue test characteristics are 4 Hz frequency and 0.1 as the ratio of minimum to maximum loading in tensile regime. It is observed that there are significant amount of continuous emissions released from the notch tip due to the formation of plastic deformation and slow crack growth. The frequency spectra of continuous emissions and burst emissions are compared to understand the difference of sudden crack growth and gradual crack growth. The predicted crack growth rate is compared with the AE data using the cumulative AE events at the notch tip. The source mechanism of sudden crack growth is obtained solving the inverse mathematical problem from output signal to input signal. The spline component of gearbox structure is a non-redundant element that requires early detection of flaws for preventing catastrophic failures. In this paper, the fatigue crack growth of a notched and flattened gearbox spline component is monitored using the AE method The AE data is continuously collected together with strain gauges. There are significant amount of continuous emissions released from the notch tip due to the formation of plastic deformation and slow crack growth. The source mechanism of sudden crack growth is obtained solving the inverse mathematical problem from output signal to input signal.

Keywords: Fatigue test, acoustic emission, spline, gear box

1. INTRODUCTION

The gearbox component is an important mechanical member of helicopters as it makes the engine torque remain at optimum levels while transmitting the power. The spline section of gearbox is a non-redundant element, and subjected to fatigue loading. Thus the spline section is susceptible to develop fatigue cracks and spalling. Therefore, it is important to understand the mechanical behavior of spline section and design nondestructive evaluation method to prevent catastrophic failures.

The development of diagnosis technique for the gearbox components is a field of research that has been active for several decades. Z. Yu et al [1] conducted the macroscopic and microscopic examination on an idler gearbox, and found typical cracks on the spline section. P. Sinha et al. [2] used a similar method to investigate the spline shaft of an under slung crane. In order to understand characteristics of mechanics, there are varieties of vibration monitoring methods, which are proposed based on the vibration signals and signal processing technique. S. T. Lin et al. [3] analyzed the vibration signal generated by a fault using the B-spline wavelet to understand the signature of spectrograms due to the crack evolution in a gear. B. Liu et al. [4] worked on diagnosing the gearbox fault using empirical mode decomposition and Hilbert spectrum aiming the vibration signal. F. Bonnardot et al. [5] proposed a method to resample the acceleration signals of gearbox, by means of their method, such that the rotation behavior was tracked. Though the vibration analysis as a well-established and common method can monitor the vibration properties of gearbox, it is mainly used for predicting the gear-mesh stiffness [6–8]. The sensitivity is usually not sufficient for spline crack especially for the initial crack; in addition, the operational conditions may cause potential influence to reduce the accurate. Acoustic emission (AE) is another passive NDE method to detect the crack in the gearbox. A. Rezaei et al. [9] proposed a new approach to prognosis the gearbox system, which is to combine the vibration and acoustic emission. The defect to failure tests were

conducted to evaluate the method, good results were obtained during idle engine performance. Y. Qu et al [10] employed acoustic emission and vibration sensors to detect the tooth faults in the gearbox, through the comparative study, the acoustic emission method shows more stable performance of detection different gear tooth damage. M. Khazaee et al. [11] used a data fusion technique of vibration and acoustic emission to detect the faults in the gearbox. F. Elasha et al. [12] detected the bearing faults using the acoustic emission, by means of AE data processing, the faulty and healthy conditions could be identified.

Although there are many studies aiming to the spline section of gearbox in a laboratory scale demonstration, the AE method is challenged by the complexity of signal, and the influence of background noise in a realistic application. The superiority of acoustic emission has not been fully used. However, similar research [13–15] on the fatigue testing of different materials can be adapted to the gearbox application. The majority studies used simple plate geometry; however, the spline section in the gearbox is quite complex, which would affect the AE signature. In this study, the fatigue test is conducted on a test sample simulating a flattened spline structure. The AE data is continuously collected to identify the signatures of the plastic deformation and crack growth. The AE data is compared with strain gauges in terms of detecting the initiation of fatigue crack growth. The AE signatures representing two source mechanisms of plastic deformation and sudden crack jump are obtained.

2. DESCRIPTION OF EXPERIMENTS

2.1 Numerical Model

The experimental setup includes recording AE and strain data continuously during the fatigue testing. In addition to the AE data, ultrasonic data is collected periodically when the specimen is under no load (before and after the test) using the array of piezoelectric patches. In this paper, only the results of AE data are presented. The schematic of the data collection strategy and experimental setup are shown Figure 1. The detailed test sample is shown in Figure 2a. The PZT array (see in Figure 2b) is mounted on the open window section of the test sample similar to actual testing of spline component. The AE data is recorded using six AE sensors: channels 1 to 3 are WD sensors (wideband sensor manufactured by Mistras Group Inc) and placed in a triangulation form for source localization; channel 4 is Nano30 sensor (nano-30 FP 97 sensor manufactured by Mistras Group Inc) and placed in the windowed section where the ultrasonic array is placed; channels 5 and 6 are PZT sensors named as B2 and B3 sensors of the ultrasonic array (see in Figure 2c). All the sensors are connected to 40 dB gain pre-amplifiers. The AE data is collected using PCI-8 data acquisition board manufactured by Mistras Group Inc. The ultrasonic signal is recorded using the data acquisition system manufactured by Metis Design Inc. Two strain gauges manufactured by Micro Measurements are positioned on the notch tip and the corner of the windowed section, respectively (see Figure 2c). The strain data is collected using National Instrument data acquisition system and Labview program. The fatigue test is performed with the Instron loading machine as shown in Figure 1. The fatigue load setting is 4 Hz frequency with max/min load ratio as 0.1, and maximum load as 12 kN.

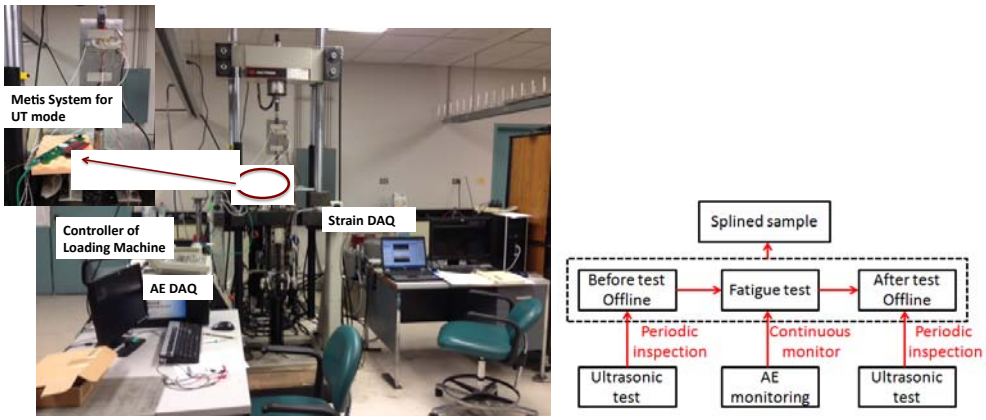

Figure 1. The experimental setup and data acquisition strategy

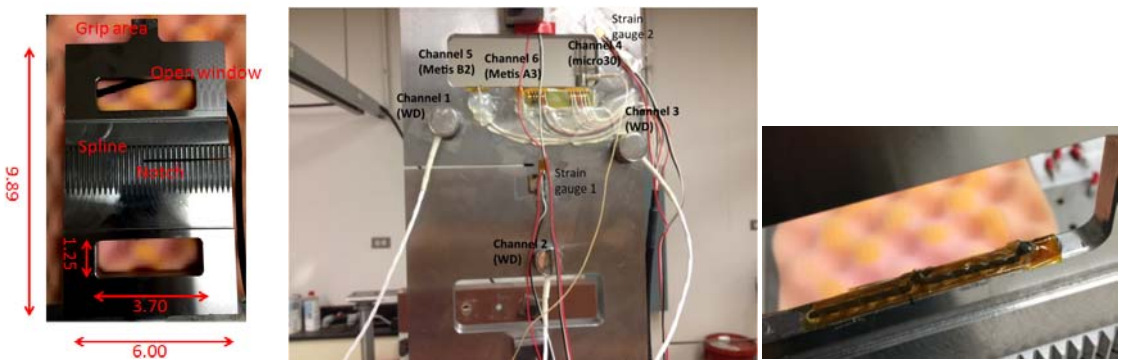

(a) (b) (c)

Figure 2. The profile of the sample and sensor setup (a) the detailed splined sample (b) the PZT wafer details(c) the sensor setup

3. FRACTURE MODEL

The tested sample is modeled using Franc3D software to identify the crack growth characteristics. Figure 3 shows the image of the predicted crack growth direction, and the stress intensity factor for 1000 lb (4.5 kN). The predicted crack growth rate for 12 kN loading is 12.7×10^{-6} mm/cycle. The crack length after about 550,000 cycles is predicted as 7 mm. The direction of crack growth obtained through Franc3D shows good agreement with experimental observation as discussed below.

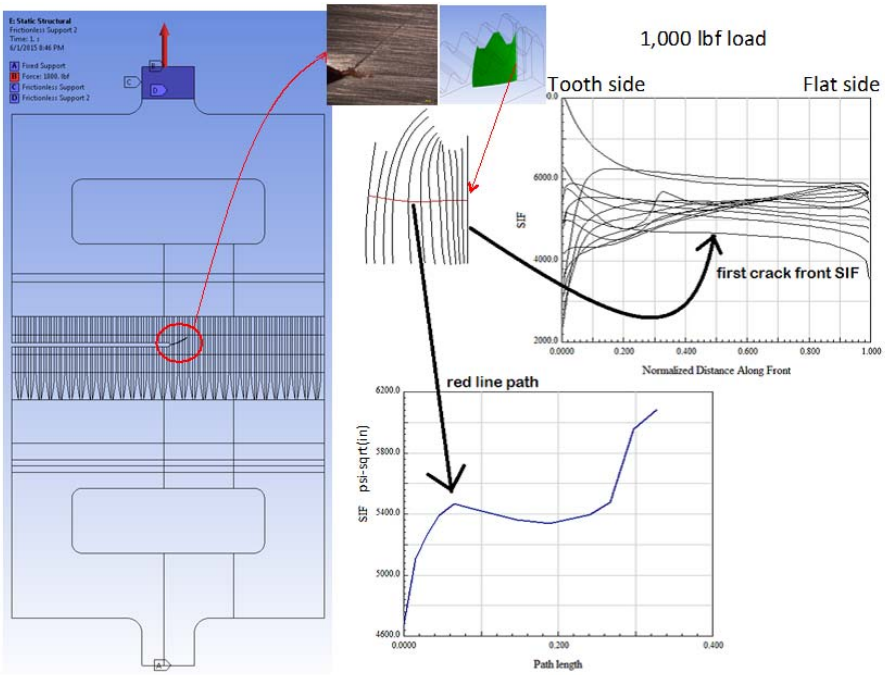

Figure 3. The Franc3D model and experimental results

4. EXPERIMENTAL RESULTS

4.1 Strain History

Figure 4 shows the minimum and maximum envelops of strain levels throughout the fatigue testing for the strain gauge 1 located near the crack tip and the strain gauge 2 located near the window edge (labeled in Figure 2). The amplitude of the strain gauge 1 increases abruptly at the end of 8/18/2015, while the strain gage 2 has stable response throughout the testing. The peak value of the strain gauge 1 occurs between 8/18/2015 and 8/20/2015, which corresponds to the fatigue cycle range of 380,068 to 484,293. The sudden increase of the strain level near the notch tip is related to the crack growth. Once the crack tip passes the strain gauge location, the surface that strain gauge is attached is exposed to the compression zone, which is also observed in the strain envelope (after 08/25/2015).

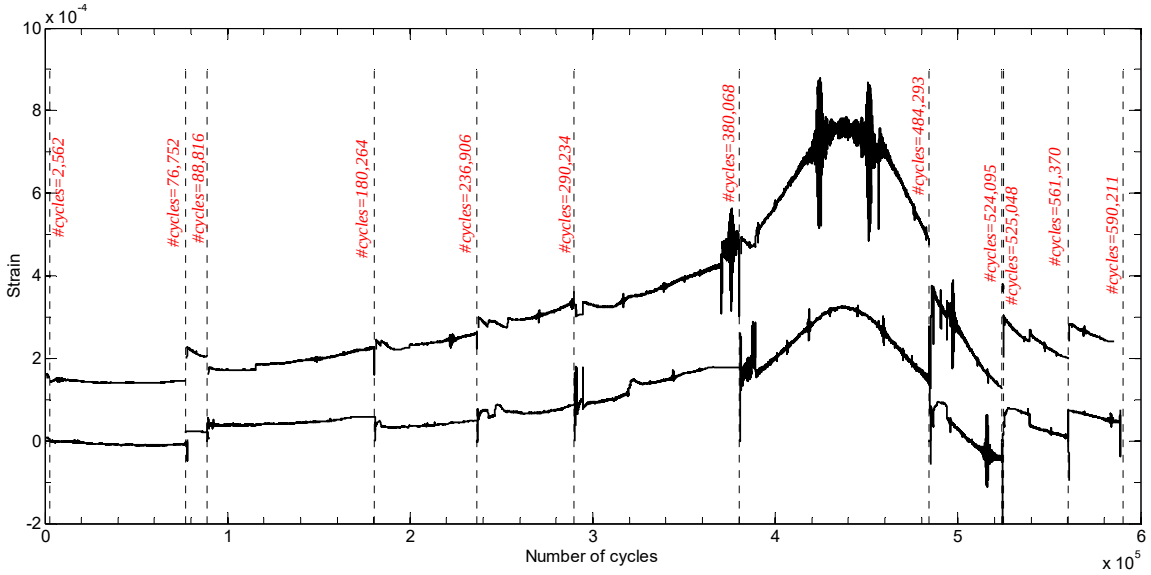

(a)

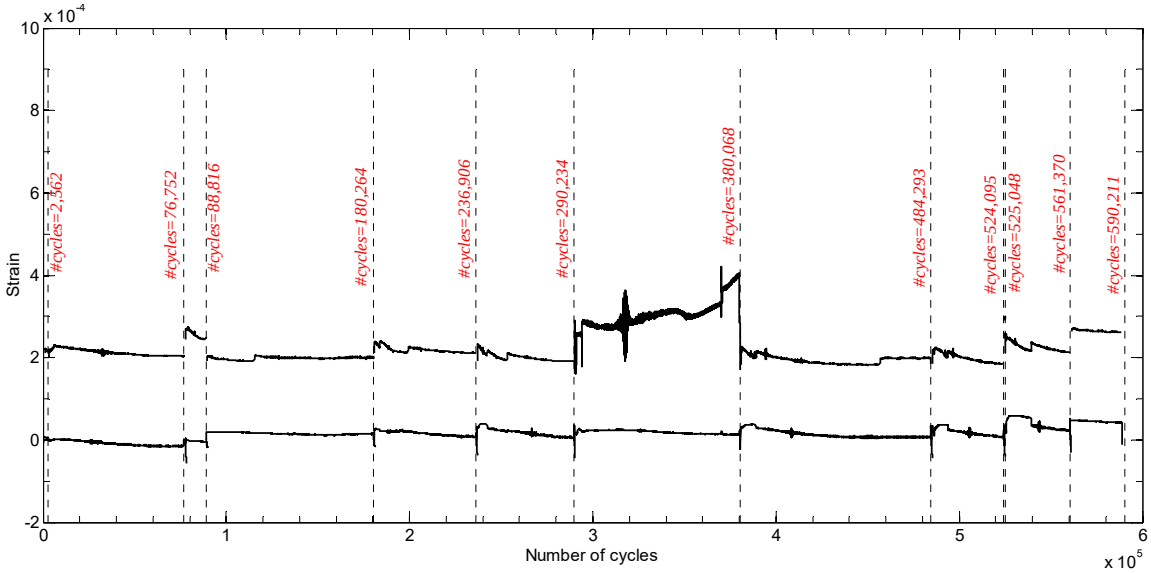

(b)

Figure 4. The strain history (a) strain gage 1 (b) strain gage 2

4.2 Crack Growth versus Cumulative AE Features

Figure 5 shows the cumulative AE events located using channels 1 to 3 versus cumulative fatigue cycles. The total AE events located near the notch tip are 128. There is a significant increase in the cumulative AE events after about 380,000 cycles, which coincides with the increase of strain near the crack tip as shown in Figure 4. The major crack growth behavior is observed between 400,000 – 500,000 cycles. A microscopic image of crack growth observed after 600,000 cycles is shown in Figure 5. The crack direction agrees with the numerical result as discussed in section 3.

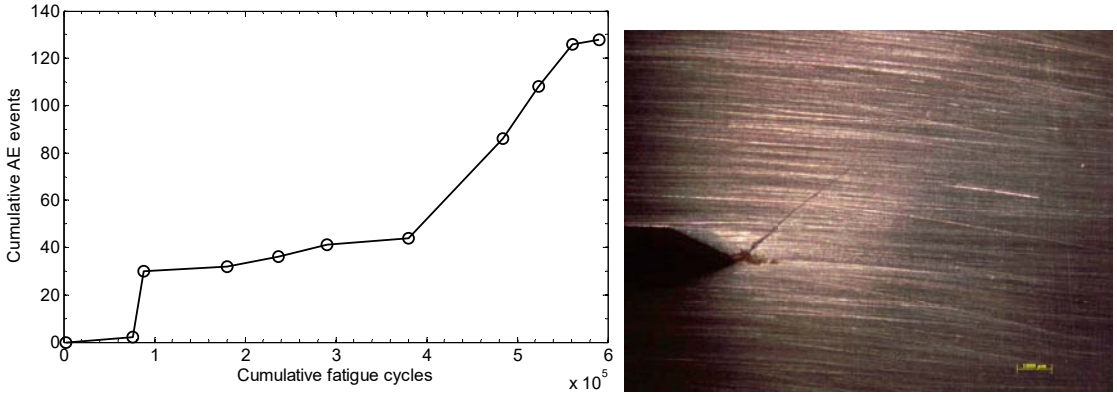

Figure 5. Cumulative AE events and cumulative fatigue cycles and microscopic image of crack growth

4.3 Examples of AE Waveforms

4.3.1 Burst Emissions from Notch Tip

Based on the observation of sections 4.1 and 4.2, an AE event located near the notch tip and occurred near 400,000 cycles is selected for further analysis. Figure 6 shows the time domain histories of all six channels detected by the same event. The output signals of sensors 5 and 6 are noisier than the other sensors. In general, Metis sensors have lower sensitivity than conventional AE sensors, which is mainly due to the miniature size, and higher noise level due to unshielded cables used. However, they detected the large crack growth event located near the notch tip. The comparison of channel 4 (nano 30) with channels 5 and 6 (Metis sensors) reveals that Metis sensors are about ten times less sensitive than nano30. However, they all detected a particular frequency near 100 kHz, Figure 7, which can be used in separating crack growth events and secondary AE sources.

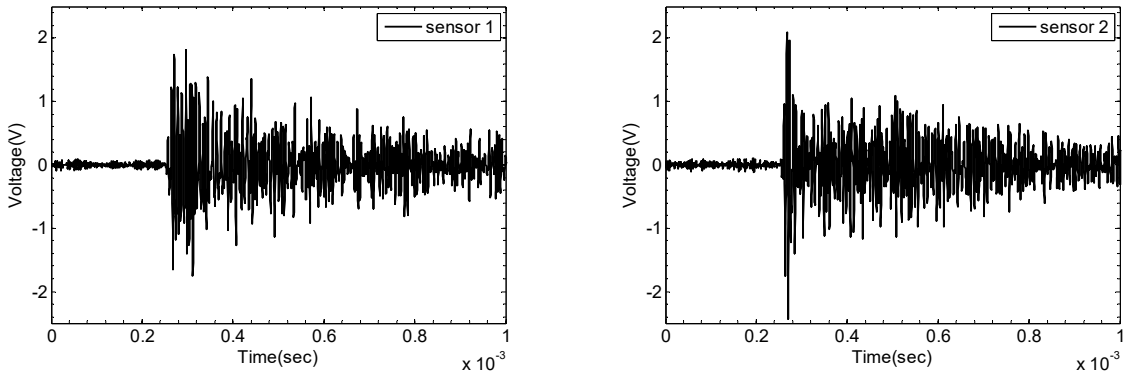

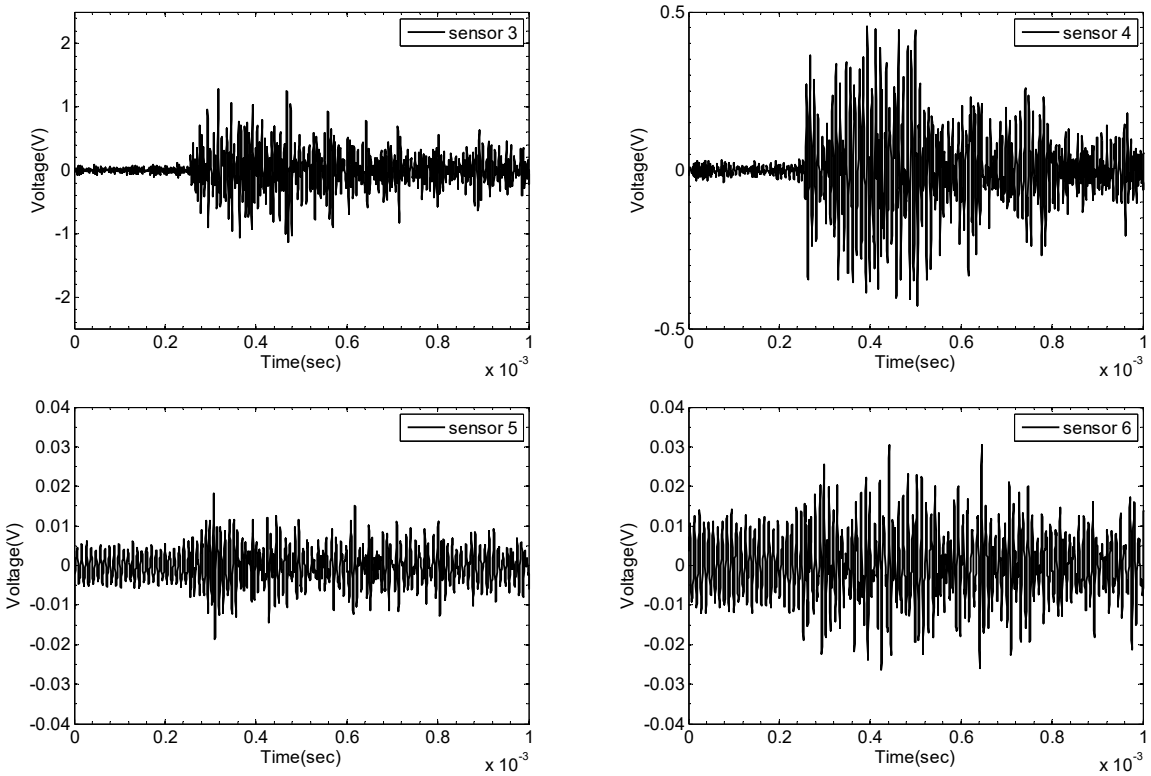

Figure 6. Time domain histories of the AE event detected by all six sensors, and located near the notch tip near 400,000 cycles

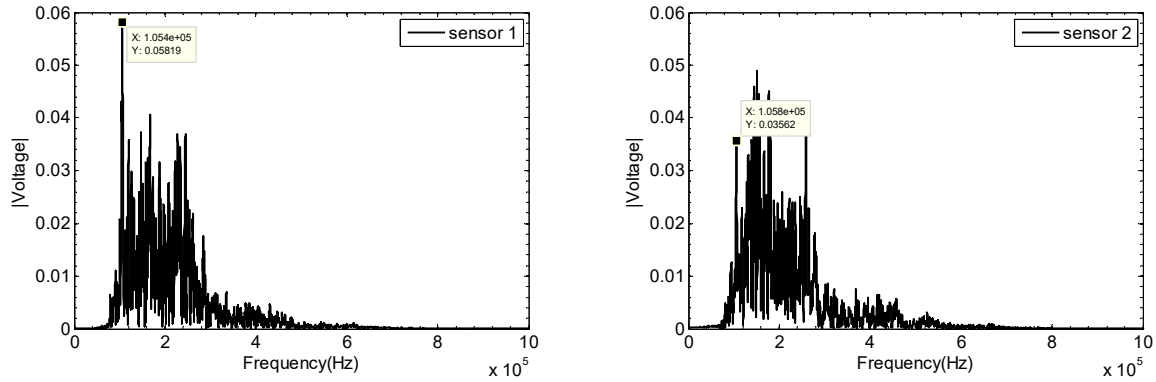

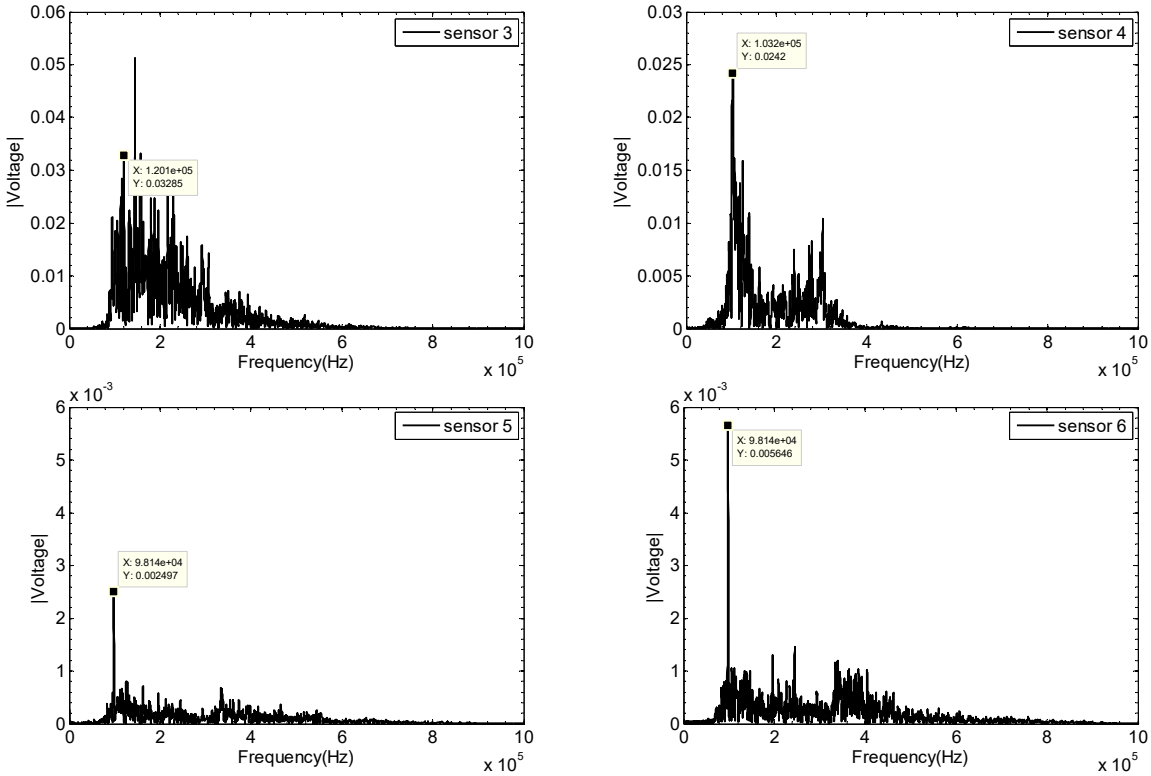

Figure 7. Frequency spectra of AE event detected by all six sensors, and located near the notch tip near 400,000 cycles

4.3.2 Continuous Emission from Notch Tip

The fatigue test was started in the mornings and ended about five to six hours of testing each day. The threshold level was initially set as 50 dB at the beginning of each testing. A pattern of increasing noise level was observed after about 237,000 cycles. The hit-rate increased significantly about 10 minutes of testing, and the threshold level was increased to 55 dB. The hit-rate increased after about 20-30 minutes of testing, and the threshold was increased to 60 dB. The hit-rate increased again significantly after 40-60 minutes of testing, and the AE data was recorded with 65 dB threshold. This behavior was repeated until the test was ended with about 7 mm crack growth. It is considered that the increase of continuous emissions from notch tip is a pre-cursor indication of sudden crack growth jumps, which generate burst type AE signals. Figure 8 and Figure 9 show time histories and frequency spectra of six examples of continuous emission signals detected by channel 3 near the peak load. There is a distinct frequency near 200 kHz. The difference of frequency characteristics of burst signals and continuous signals can be utilized to separate different source mechanisms. Additionally, typical gearbox operation noise generates signal below 100 kHz. The initiation of plastic deformation can be deduced from the AE signal if the sensors are positioned close proximity to the location of crack growth.

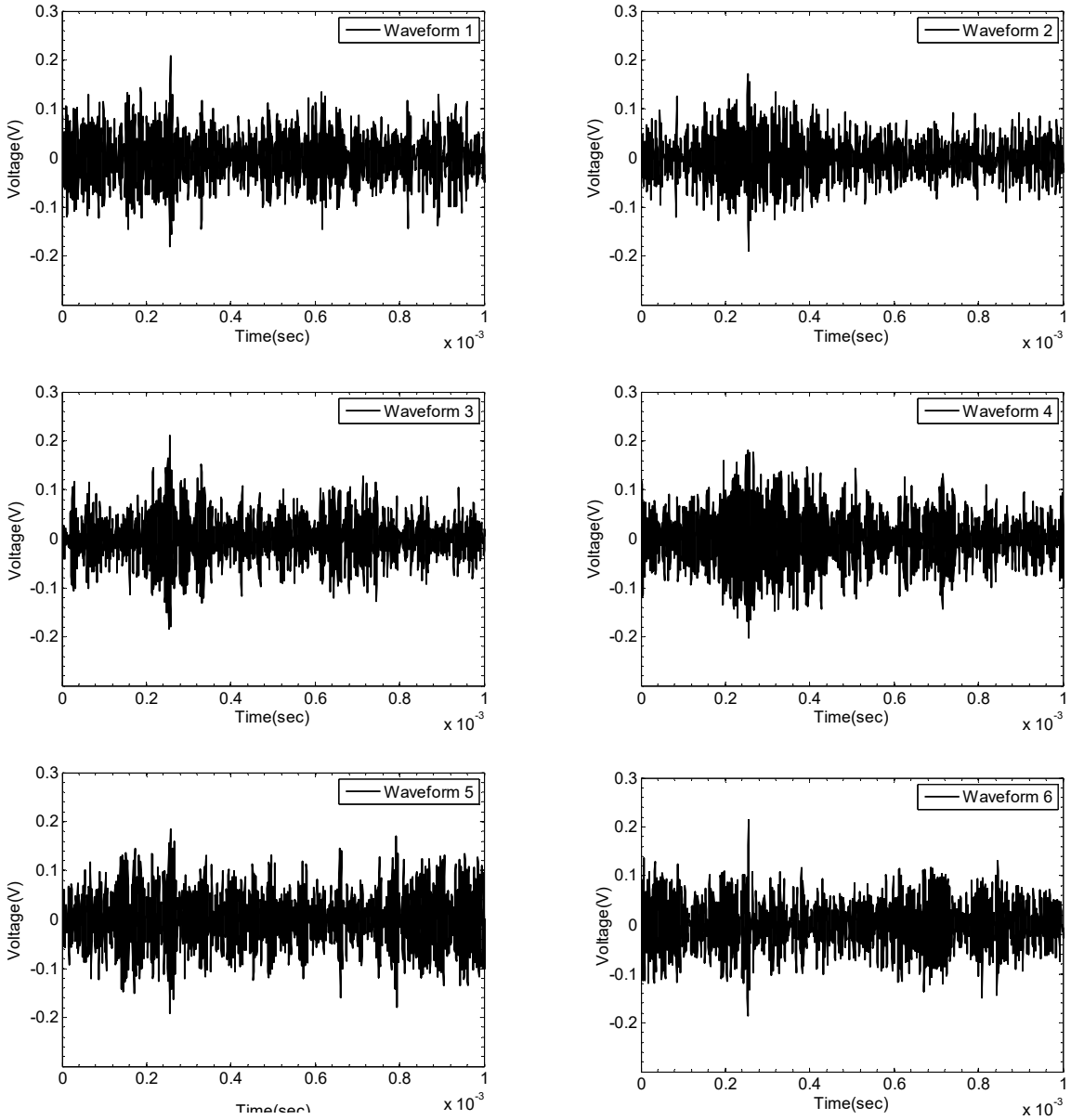

Figure 8. Examples of continuous emission signal detected by CH3 (across the notch tip)

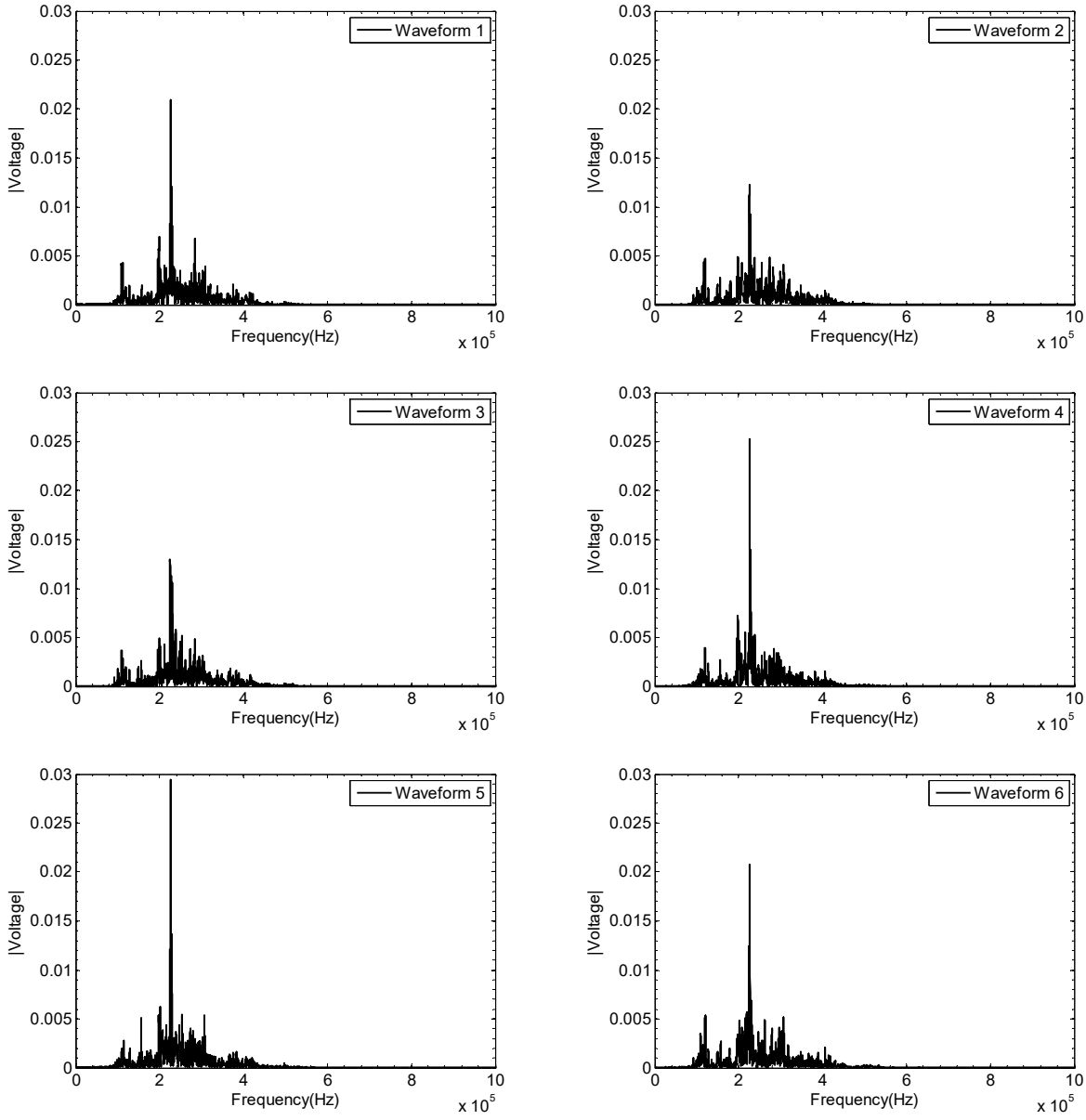

Figure 9 Frequency spectra of continuous emission signals detected by sensor 3 (WD sensor)

4.3.3 Comparison of Burst and Continuous Emission

A distinct difference between the frequency spectra of burst and continuous emission is observed. Examples of burst and continuous AE signals are selected, their AE characteristics including peak frequency, amplitude, and frequency centroid are extracted and shown in Table 1. In general, the burst signals have lower peak frequency and frequency centroid than the continuous signals. The AE amplitude does not indicate any distinct difference between two signal types. The other time domain features such as duration and rise time have no meaning for continuous type signals. Therefore, frequency domain features are needed to separate AE source mechanisms.

Table 1. AE features of selected burst and continuous AE signals

# Day (burst/continuous)	Burst Signals				Continuous Signals			
Peak frequency (kHz)	119.3	119.2	112.6	188.7	226.0	113.7	225.7	226.5
Amplitude (mV)	31.48	14.4	26.3	14.0	11.97	20.80	16.43	15.59
Frequency centroid (kHz)	236.8	286.2	242.1	271.3	250.8	273.9	272.5	303.3

5. CONCLUSIONS

In this paper, the gearbox spline geometry is simulated with a simplified model in order to test the structure under fatigue testing. The spline details and thickness are preserved while the circular geometry is simplified to a flat surface. The ultimate goal is to understand the AE characteristics of crack growth that can be adapted to the pattern recognition approach of a realistic test stand. The crack size reached about 7 mm about 600,000 cycles, which is confirmed by the numerical model. While there were limited number of burst type signals detected near the notch tip, significant amount of continuous signals are observed. It is confirmed that the continuous signals are released as a result of mechanism at the notch tip based on the hit sequence of AE sensors. The AE sensor close proximity to the notch tip is the first hit channel of continuous AE signals presented in this study. Continuous and burst signals have distinct frequency spectra while time domain features have similar characteristics. In future work of this study, the experimental results will be adapted to the AE data recorded from a realistic test stand at NAVAIR facility.

ACKNOWLEGMENT

This material is based upon work supported by the U.S. Naval Air Systems Command (NAVAIR) under Contract No. N68335-13-C-0417 entitled "Hybrid State-Detection System for Gearbox Components" awarded to the Metis Design Corporation. Any opinions, findings and conclusions or recommendations expressed in this material are those of the authors and do not necessarily reflect the views of NAVAIR.

REFERENCES

[1] Z. Yu, X. Xu, Failure analysis of a diesel engine crankshaft, Eng. Fail. Anal. 12 (2005) 487–495. doi:10.1016/j.engfailanal.2004.10.001.

[2] P. Sinha, S. Bhattacharyya, Failure investigation of spline-shaft of an under slung crane, J. Fail. Anal. Prev. 13 (2013) 601–606. doi:10.1007/s11668-013-9719-9.

[3] S.T. Lin, P.D. McFadden, Gear vibration analysis by B-spline wavelet-based linear wavelet transform, Mech. Syst. Signal Process. 11 (1997) 603–609. doi:10.1006/mssp.1997.0097.

[4] B. Liu, S. Riemenschneider, Y. Xu, Gearbox fault diagnosis using empirical mode decomposition and Hilbert spectrum, Mech. Syst. Signal Process. 20 (2006) 718–734. doi:10.1016/j.ymssp.2005.02.003.

[5] F. Bonnardot, M. El Badaoui, R.B. Randall, J. Danière, F. Guillet, Use of the acceleration signal of a gearbox in order to perform angular resampling (with limited speed fluctuation), Mech. Syst. Signal Process. 19 (2005) 766–785. doi:10.1016/j.ymssp.2004.05.001.

[6] Y. Pandya, A. Parey, Failure path based modified gear mesh stiffness for spur gear pair with tooth root crack, Eng. Fail. Anal. 27 (2013) 286–296. doi:10.1016/j.engfailanal.2012.08.015.

[7] Z. Li, X. Yan, Z. Tian, C. Yuan, Z. Peng, L. Li, Blind vibration component separation and nonlinear feature extraction applied to the nonstationary vibration signals for the gearbox multi-fault diagnosis, Measurement. 46 (2013) 259–271. doi:10.1016/j.measurement.2012.06.013.

[8] A.B. Andhare, M.K. Verma, Vibration Engineering and Technology of Machinery, 23 (2015) 1091–1100. doi:10.1007/978-3-319-09918-7.

[9] A. Rezaei, A. Dadouche, Development of a turbojet engine gearbox test rig for prognostics and health management, Mech. Syst. Signal Process. 33 (2012) 299–311. doi:10.1016/j.ymssp.2012.05.013.

[10] Y. Qu, D. He, J. Yoon, B. Van Hecke, E. Bechhoefer, J. Zhu, Gearbox tooth cut fault diagnostics using acoustic emission and vibration sensors--a comparative study., Sensors (Basel). 14 (2014) 1372–1393. doi:10.3390/s140101372.

[11] M. Khazaee, H. Ahmadi, M. Omid, A. Moosavian, M. Khazaee, Classifier fusion of vibration and acoustic signals for fault diagnosis and classification of planetary gears based on Dempster-Shafer evidence theory, Proc. Inst. Mech. Eng. Part E-Journal Process Mech. Eng. 228 (2014) 21–32. doi:Doi 10.1177/0954408912469902.

[12] F. Elasha, M. Greaves, D. Mba, A. Addali, Application of Acoustic Emission in Diagnostic of Bearing Faults within a Helicopter Gearbox, Procedia CIRP. 38 (2015) 30–36. doi:10.1016/j.procir.2015.08.042.

[13] G. a. Bigus, a. a. Travkin, An evaluation of the flaw-detection characteristics for the detection of fatigue cracks by the acoustic-emission method in samples made of steel 20 that have a cast structure, Russ. J. Nondestruct. Test. 51 (2015) 32–38. doi:10.1134/S1061830915010027.

[14] C.K. Mukhopadhyay, T. Jayakumar, T.K. Haneef, S. Suresh Kumar, B.P.C. Rao, S. Goyal, et al., Use of acoustic emission and ultrasonic techniques for monitoring crack initiation/growth during ratcheting studies on 304LN stainless steel straight pipe, Int. J. Press. Vessel. Pip. 116 (2014) 27–36. doi:10.1016/j.ijpvp.2014.01.005.

[15] J. Yu, P. Ziehl, Stable and unstable fatigue prediction for A572 structural steel using acoustic emission, J. Constr. Steel Res. 77 (2012) 173–179. doi:10.1016/j.jcsr.2012.05.009.